Advanced Science Letters
Volume 15, Pages 417–421 (August 2012)

Preparation and Characterization of Porous Nano Copper Films

Huijun Zhang, Mingyu Li*, Qingxuan Zeng, and Changgen Feng

School of Mechatronical Engineering, Beijing Institute of Technology, Beijing 100081, P. R. China

Nanocrystalline porous copper films were prepared by sol–gel method with polyethylene glycol (PEG) as organic template, copper acetate as raw material and (di) ethanolamine (DEA) as chelating agent. Copper nanowire array films were fabricated by electrodeposition within anodic aluminum oxide (AAO) membrane. The films were analyzed by infrared absorption (IR), thermogravimetry-derivative thermogravimetry (TG-DTG), X-ray diffraction (XRD), energy dispersive X-ray spectroscopy (EDX), scanning electron microscope (SEM) and atomic force microscope (AFM). The structure of the copper films which achieved by sol–gel was remarkable influenced by sol concentration, polyethylene glycol content and annealing temperature. The effects of annealing temperature and the way of gelation on grain sizes were discussed. The results showed that films could be made under the optimum condition: sol concentration was 0.6 mol/L, annealing temperature was 500 °C, and polyethylene glycol content was 0.35 g. The structure of the nanoarray films which obtained by electrodeposition was influenced by current density and electrodeposition time. When the electrodeposition time was 5 min, and current density was 1.0 A/dm^2, the nanoarray structure was the best.

Keywords: Porous, Nano, Film, Sol–Gel, Electrodeposition.

1. INTRODUCTION

Porous metals were developed quickly in these years because of their good permeability, good thermal stability, corrosion resistance and high strength. There are a lot of connected pores in it, and metal nanoparticles. Therefore, the nanoporous metal materials have extensive application prospects in catalytic, filtration, surface plasmon resonance, sensing, heat exchange, drug transport for their high specific surface area, lightweight, savings in raw materials and other characteristics.[1]

Template method is the main method for preparing the porous nano-metal materials.[2] The template is immersed in the metal salts solution or metal colloid solution. The metal is loaded on the template through certain technology, and the porous metal could be achieved when the template is removed by annealing, corrosion or dissolution. This method has good controllability, and it is widely used in the preparation of highly ordered nano-porous metal materials.[3] The main technologies for template synthesis are magnetron sputtering,[4] electrodeposition,[5–7] and sol–gel method.[8, 9]

In this paper, porous nano copper films were prepared by sol–gel method with PEG as template. Highly ordered nanoarray films were prepared by electrodeposition method with AAO as template. We did some research on different experimental conditions, which would affect the structure of the film. We also obtained some valuable results.

*Author to whom correspondence should be addressed.

2. EXPERIMENTAL DETAILS

2.1. Sol–Gel Method

$Cu(CH_3COO)_2 \cdot H_2O$ was dissolved in isopropyl alcohol. The solution was stirred by a magnetic stirrer at 50 °C. Then (di)ethanolamine ($HN(CH_2CH_2OH)_2$, DEA) was added in two times of copper ion concentration. When the mixture was completely clear, water (H_2O/Cu acetate, 1:1 mol) and polyethylene glycol (PEG, $H(OCH_2CH_2)_nOH$) were added to the resulting solution. Two hours later, a stable and dark blue sol was obtained. The sol was aged for 24 h at room temperature. Films were prepared by spin coating. The solution was spreaded on the substrate at 800 rpm for 18 s and 2000 rpm for 30 s. Afterwards, the films were dried at 100 °C for 10 min following deposition of each layer. At last, films were placed in a furnace and annealed in N_2. The furnace temperature was raised with a heating rate of 3 °C/min and held at a certain temperature for 1 h.

2.2. Electrochemical Deposition Method

A copper layer was sputtered on one side of the AAO template (70∼80 nm pore-diameter), and served as the working electrode. Pure red copper plate was used as the anode. The plating solution containing 70 g/L $CuSO_4 \cdot 5H_2O$ and 80 ml/L H_2SO_4 was used to prepare copper nanowire array. All experiments were carried out at room temperature without stirring. At last, the samples were washed by deionized water and immersed in 5% NaOH solution for 30 min to remove the AAO template. Then nanowire array films were achieved.

2.3. Representation

The IR absorption spectra of sol–gel process were achieved by infrared spectrometer (TENSOR 27). The surface morphologies of films were examined by SEM (Hitachi S-4700) and AFM (CSPM5500). TG-DTG analysis of dried gel was obtained by thermal analyzer (SII TG/DTA6300). The EDX spectrum of the film was achieved by energy dispersive X-ray detector (Horiba EMAX EX350). The crystal structure and the crystallization behavior of the films were analyzed by XRD (D8 ADVANCE).

3. RESULTS AND DISCUSSION

3.1. Infrared Absorption Spectra of Sol–Gel Process

Figure 1 is the IR spectra of sol–gel process. Curve (1) in Figure 1 indicates the standard peaks of DEA. Curve (2) is the IR spectrum of $Cu(CH_3COO)_2 \cdot H_2O$. The peaks at 3000–3500 cm^{-1} are assigned to the stretching vibrations of O—H species. The peak at 1602 cm^{-1} indicates C═O species and the peak at 1445 cm^{-1} indicates CH_2 species. Curve (3) is the IR spectrum of dried gel. The peak at 3253 cm^{-1} indicates N—H species, and the peaks at 2925 and 2871 cm^{-1} are assigned to the C—H stretching vibrations of DEA. It indicates that $[CH3COOCu]^+$ has formed in this process. Meanwhile, the diagnostic peak of N—H at 3418 cm^{-1} weakens in the curve (3), and the peaks of C-N at 1122 cm^{-1} also weakens. It shows that the stable metal complex compound has formed between $Cu(CH_3COO)_2 \cdot H_2O$ and DEA.

3.2. Thermal Analysis of Dried Gel

Figure 2 shows TG-DTG curves of the dried gel. The TG curve can be divided into four stages: The first stage is from room temperature to 150 °C. The quality loss is about 8%, and it should be due to the evaporation of water and isopropanol. The second stage is 150∼250 °C, and quality loss is about 54%, corresponding to the combustion of PEG and DEA. The third stage is 250∼500 °C, and the quality loss is about 20%. It should be due to the combustion of residual organics. The last stage is 500∼650 °C. There is no further weight loss in this stage. So it can be initially determined that the annealing temperature is 500 °C.

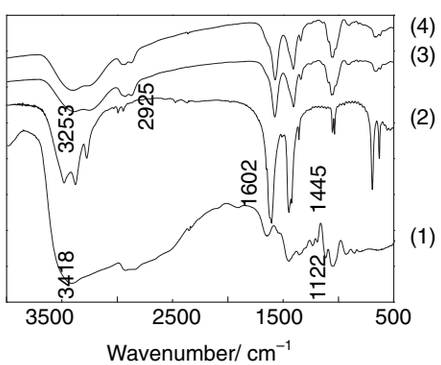

Fig. 1. Infrared absorption spectra of sol–gel process. (1) DEA (2) $Cu(CH_3COO)_2 \cdot H_2O$ (3) DEA + $Cu(CH_3COO)_2 \cdot H_2O$ + H_2O + $(CH_3)_2CHOH$ (4) DEA + H_2O + $(CH_3)_2CHOH$ + $Cu(CH_3COO)_2 \cdot H_2O$ + PEG1000.

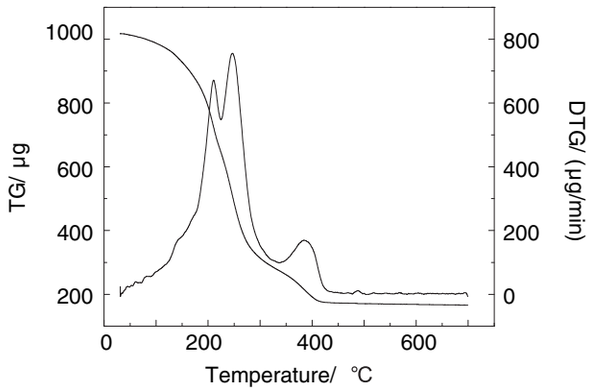

Fig. 2. Thermal analysis of dried gel.

3.3. Composition Analysis of Film

Figure 3 shows XRD patterns of the films which were achieved by sol–gel method. The films were annealed at different temperatures in nitrogen. Three reflections at $2\theta = 43.45°$ (111), 50.56° (200) and 74.16° (220) were observed in the diffraction patterns and ascribed to the formation of the copper monoclinic crystal phase. As the annealing temperature increases, diffraction peak narrows down, diffraction intensity increases, and half peak reduces. When the films were annealed under 400, 450, 500 and 550 °C, the average grain sizes of the films are 34.83, 41.25, 49.45 and 52.51 nm calculated by the *Scherrer*.

Figure 4 shows EDX spectrum of the film which was achieved by electrodeposition method. The EDX data show that the mass percent of copper is 96.82%. It confirms that pure copper films were obtained. But the film also contains oxygen element. It may come from organics that have not been completely removed. It is also possible that the nano copper films were oxygenated.

3.4. Surface Morphologies Analysis by Scanning Electron Microscope

Figure 5 shows that SEM photographs of copper films which were obtained with different sol concentrations. Surface crack is detected when the concentration reached a particular level. Since the viscosity of sol–gel increases, the coating thickness of the each film continuously increases. The internal stress in membrane which is produced by drying also strengthens gradually. When the stress intensity overwhelms the bond strength of the film,

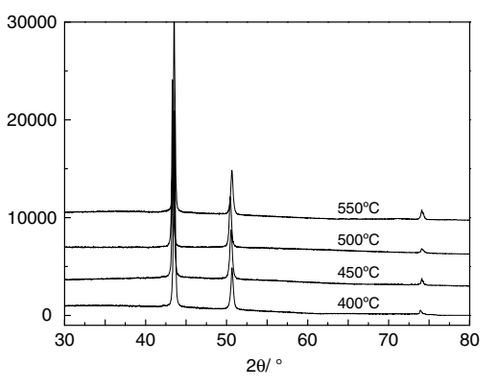

Fig. 3. X-ray diffraction patterns of porous film.

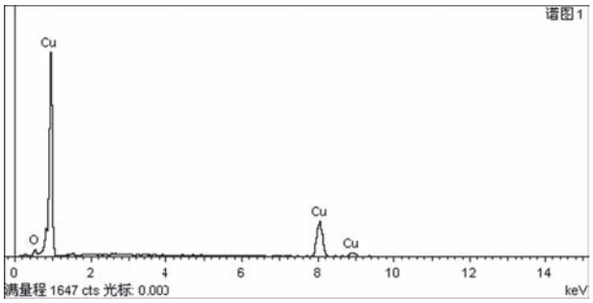

Fig. 4. Energy dispersive X-ray spectrum of nanoarray film.

the film will crack or even be peeled off. It is visible that when the sol concentration was 0.6 mol/L, the feature of the film is the best.

Figure 6 shows SEM images of the films which were prepared by sol–gel with different annealing temperatures. From the figures, we can find that the porous structure has not been formed at 400 °C. It indicates that the organics were just partly removed. While at 450 °C, the porous structure is more obvious but not fully formed, because there is a small amount of organic residue in the sample. As the temperature was raised, the organics burned gradually. So the pores are more obvious and uniform when the film was annealed at 500 °C. But at 550 °C, the porous structure was incomplete. Therefore, we can concern that the best annealing temperature is 500 °C.

Figure 7 shows SEM photographs of the films which were made by sol–gel with different amount of PEG. As it can be seen from the graph that porous structure can be formed when PEG was added in, and the film was pyknotic if there was no PEG. The pore size increases gradually with the amount of PEG increases. When the amount of PEG was 0.35 g, the pore density of the film is homogeneous with the pore size of 1∼2 μm.

The structure of PEG molecule is jagged and of long chain. When the PEG molecule dissolve in alcohol, the shape of long chain are twisty. PEG can enwrap granules and connect particles in sol, and the porous structure is formed by mechanism of phase separation. Oxygen atom in PEG molecule and sol particles are dominated by hydrogen bonding, and repelling force between

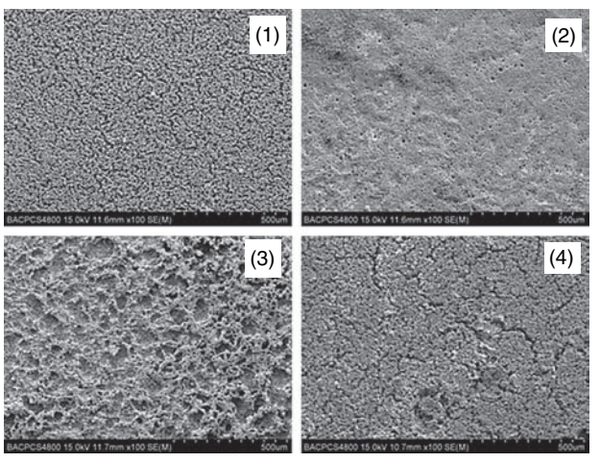

Fig. 5. Influence of porous structure from sol concentration. (1) 0.4 mol/L (2) 0.6 mol/L (3) 0.8 mol/L (4) 1.0 mol/L.

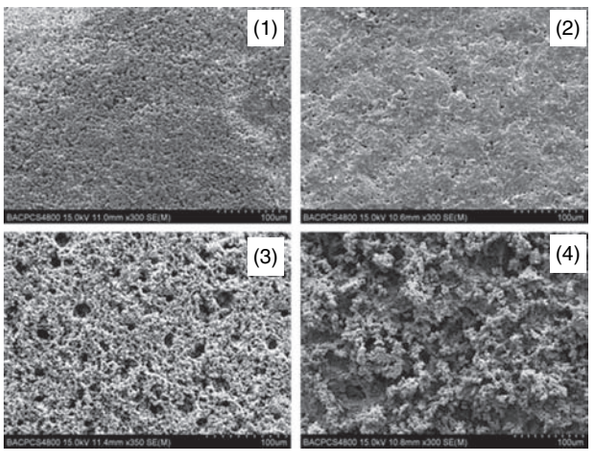

Fig. 6. Influence of porous structure from annealing temperture. (1) 400 °C (2) 450 °C (3) 500 °C (4) 550 °C.

the polymer and solvent make the two phase separated. Porous structure can be obtained when the speed of gelatination is equal or less than the speed of phase separation. By contrast, the films have few holes. So there is no obvious phase splitting when the dosage of PEG is small, for it cannot totally enwrap the granules. While the dosage of PEG is too big, the bonding between sol particles and PEG molecules is not stronger than that between the two PEG molecules. Therefore, many PEG molecules combine to form macromolecule and separate out. PEG fails to be a template, and no porous structure can be found in the film.[10]

Figure 8 shows SEM photographs of crystalline grain of the films which were achieved by sol–gel with different annealing temperatures. It can be seen that the grain size increases with the rise of annealing temperature. The crystals obtain more energy at a higher temperature, and that will contribute to the growth of crystals. When the films were annealed at 400 °C, there are a lot of organics, and the grain size is just about 25∼50 nm. At 450 °C, the grain size is 30∼60 nm, and a small amount of organic residues exist. At 500 °C, the nanoparticles are in good dispersion and uniform in size of 50∼80 nm. At 550 °C, the grain size of the films increases to 80∼100 nm.

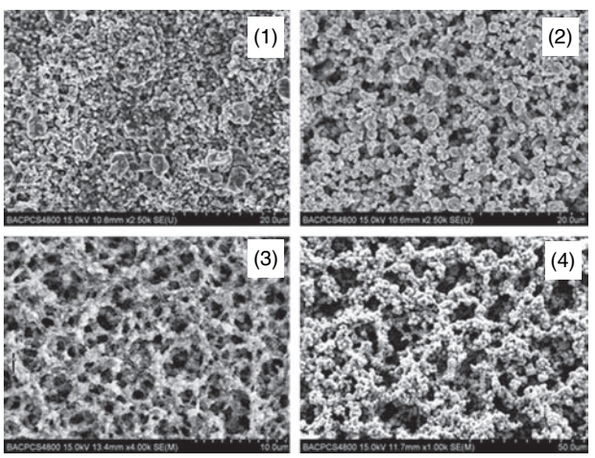

Fig. 7. Influence of porous structure from template addition. (1) 0 g (2) 0.15 g (3) 0.35 g (4) 0.45 g.

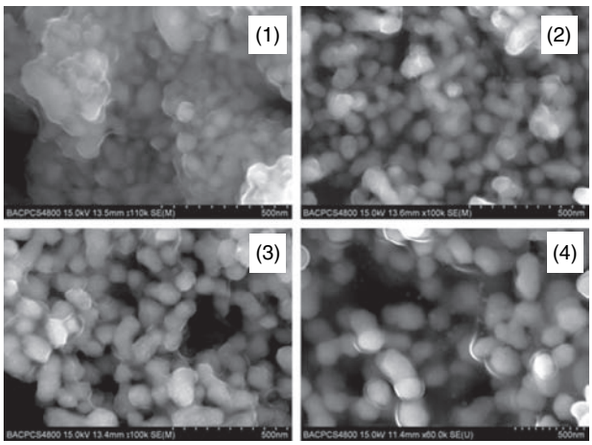

Fig. 8. Influence of grain size from annealing temperature. (1) 400 °C (2) 450 °C (3) 500 °C (4) 550 °C.

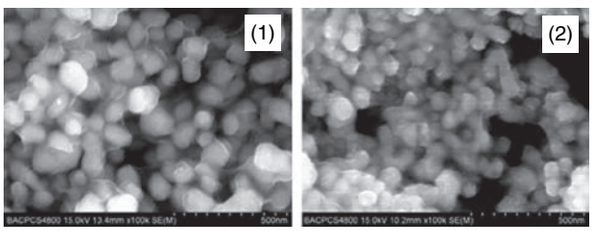

Fig. 9. Influence of grain sizes from the way of gelation. (1) aging for 24 h at room temperature (2) solvent evaporation for 2 h.

Solvent evaporation and ageing at room temperature are the main ways of the transition from sol to gel. Figure 9 shows that SEM photographs of grain sizes of the films which were influenced by the way of gelation. It can be seen that when the sol was aged for 24 h at room temperature, the grain sizes are about 50–80 nm. While the sol was evaporated for 2 h, the grain sizes of the films are about 30–50 nm. It is because that the binding force between particles can be decreased by the evaporation of the solvent, so the agglomeration of the particles is decreased. The shortening of the gelating time also could reduce the possibility of the particles coalescence. In the ageing process, the low

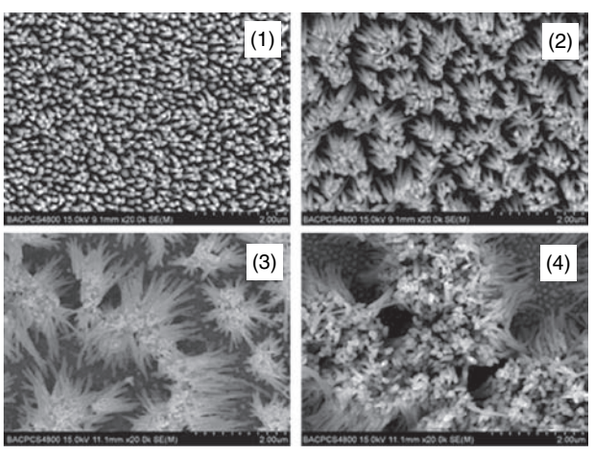

Fig. 10. Influence of nanoarray structure from current density. (1) 0.5 A/dm^2 (2) 1.0 A/dm^2 (3) 1.5 A/dm^2 (4) 2.0 A/dm^2.

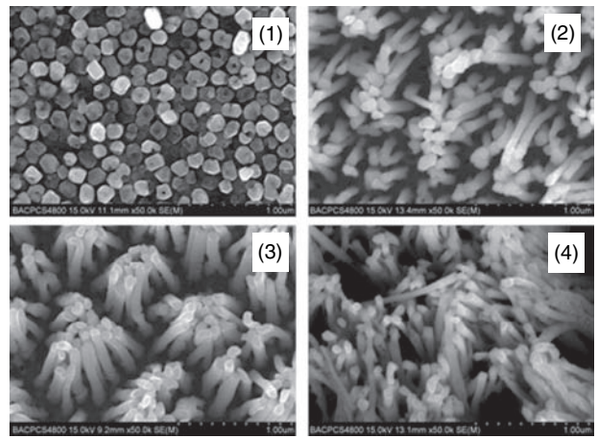

Fig. 11. Influence of nanoarray structure from electrodeposition time. (1) 1 min (2) 5 min (3) 10 min (4) 20 min.

temperature, slow reaction rate and too long gelating time can increase the possibility of the particles coalescence. The particles are apt to combine by hydrogen bonding, and the coalescence will occur in the drying and calcining stages. So the grain size is larger when the sol is aged at room temperature.

Figure 10 shows SEM images of the samples which were prepared by electrodeposition with different current densities. It can be seen that when the current density was 0.5 A/dm^2, the nanoarray structure is highly ordered, but the length of nanowire is only 600 nm. While the current density increased to 1.0 A/dm^2, the length of nanowire is 1000 nm, and the adhesion of nanowires is not observed. As the current density increases continuously, the nanowires get together and form clusters. When the current density increased to 2.0 A/dm^2, more nanowires gather and the interspace of each nanowire becomes smaller. Therefore, the best nanoarray structure can be achieved when the current density is 1.0 A/dm^2.

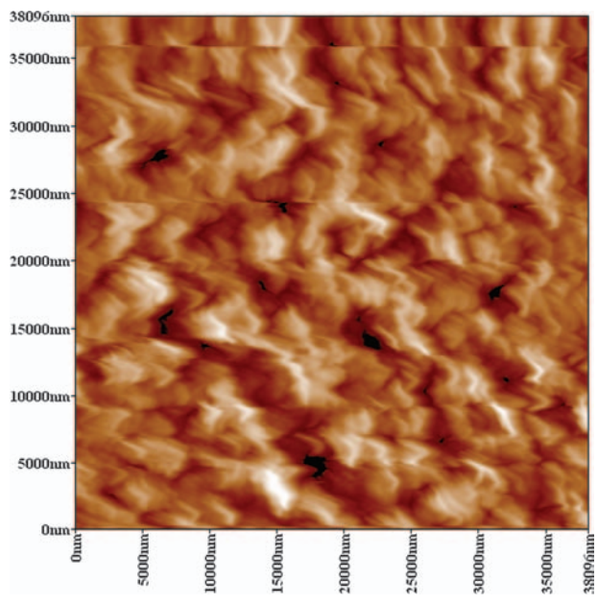

Fig. 12. Two dimension image of porous film.

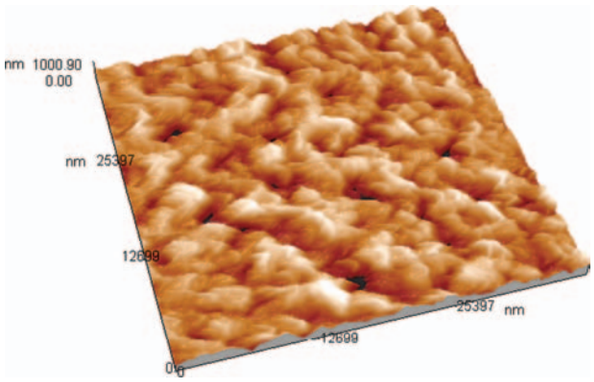

Fig. 13. Three dimension image of porous film.

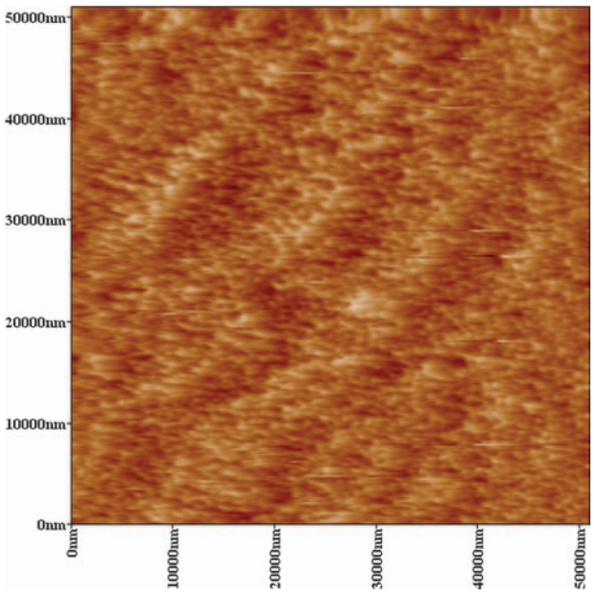

Fig. 14. Two dimension image of nanoarray film.

Figure 11 shows SEM images of the samples which were obtained by different electrodeposition times. It indicates that when the electrodeposition time was 1 min, the length of nanowires is 300 nm without any interspace. As the increasing of electrodeposition time, the length of nanowires increases accordingly. While the time increased to 20 min, more and more nanowires gather. So the optimum electrodeposition time was 5 min, and the nanowires are parallel to each other with interspace.

3.5. Surface Morphologies Analysis by Atomic Force Microscope

Two dimension and three dimension AFM images of the films which were prepared by sol–gel method are shown in Figures 12 and 13. The observation interval is 38 μm × 38 μm. We can see that the porous structure is obvious and the surface of the copper film is uneven. Copper particles are spherical and uniform in size. The analysis shows that the roughness of the surface is 125 nm and the pore size is about 1.2 μm.

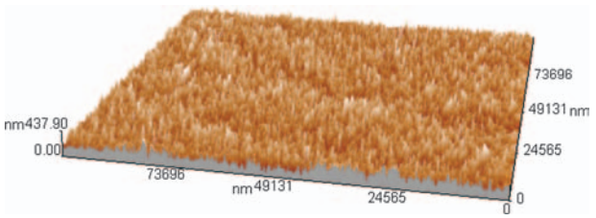

Fig. 15. Three dimension image of nanoarray film.

Two dimension and three dimension AFM images of the nanoarray films which were prepared by electrodeposition method are shown in Figures 14 and 15. We can see that there is no abnormal large particle exists. The surface of the film is accumulated with copper nanowires. The copper particles are small in size and the roughness of the surface is 58 nm.

4. CONCLUSION

Two different porous copper films were prepared by sol–gel and electrodeposition. Sol concentration, annealing temperature and PEG content had effects on porous structure of the films which achieved by sol–gel. The porous films were prepared by the optimum condition: sol concentration was 0.6 mol/L, annealing temperature was 500 °C, and PEG content was 0.35 g. The grain size of the films can be controlled by annealing temperature and the way of gelation. Solvent evaporation is a good way to decrease the grain size of the films. The grain size of the film was about 30–50 nm. The nanoarray structure obtained by electrodeposition was influenced by current density and electrodeposition time. When the current density was 1.0 A/dm^2 and electrodeposition time was 5 min, the best nanoarray films were prepared. The nanowires were parallel to each other with the diameter of 70∼80 nm.

Acknowledgments: The Committee of ICAMMP 2011 acknowledges the support from American Scientific Publisher for publishing the accepted paper in Advanced Science Letters. The financial support of the General Armament Department of PLA (No. 9140A0507111BQ0107) and the Basic Research Foundation of Beijing Institute of Technology (No. 20100242019) are gratefully acknowledged.

References and Notes

1. W. Y. Zhang, Z. P. Xi, M. Fang, Y. N. Li, G. Z. Li, and L. Zhang, *Rare Metal Materials and Engineering* 37, 1129 **(2008)**.
2. W. Liu, W. Zhong, and Y. W. Du, *Journal of Materials Science and Engineering* 25, 476 **(2007)**.
3. B. C. Tappan, S. A. Steiner, III, and E. P. Luther, *Angew. Chem. Int. Ed.* 49, 2 **(2010)**.
4. Z. Y. Ling, S. S. Chen, J. C. Wang, and Y. Li, *Chin. Sci. Bull.* 53, 183 **(2008)**.
5. T. Gao, G. W. Meng, J. Zhang, Y. W. Wang, C. H. Liang, J. C. Fan, and L. D. Zhang, *Appl. Phys. A* 73, 251 **(2001)**.
6. I. Z. Rahman, K. M. Razeeb, M. A. Rahman, and Md. Kamruzzaman, *Journal of Magnetism and Magnetic Materials* 262, 166 **(2003)**.
7. G. J. Song, X. R. Li, Y. Q. Wang, Z. Peng, Y. M. Yu, and P. D. Li, *Materials Characterization* 61, 371 **(2010)**.
8. A. Y. Oral, E. Mensur, M. H. Aslan, and E. Basaran, *Materials Chemistry and Physics* 83, 140 **(2004)**.
9. B. Guo, Z. L. Liu, L. Hong, and H. X. Jiang, *Surface and Coatings Technology* 198, 24 **(2005)**.
10. Z. F. Liu, Z. G. Jin, T. P. Xiu, W. Li, L. R. Yang, and S. J. Bu, *Rare Metal Materials and Engineering* 34, 669 **(2005)**.

Received: 12 April 2011. Accepted: 15 June 2011.